

Effects of hydrostatic pressure on Raman scattering in Ge quantum dots

K. L. Teo,^{1,*} L. Qin,² I. M. Noordin,¹ G. Karunasiri,¹ Z. X. Shen,² O. G. Schmidt,³ K. Eberl,³ and H. J. Queisser^{1,3}

¹Department of Electrical and Computer Engineering, National University of Singapore, Singapore 119260

²Department of Physics, National University of Singapore, Singapore 119260

³Max-Planck-Institut für Festkörperforschung, Heisenbergstrasse 1, 70569 Stuttgart, Germany

(Received 16 August 2000; revised manuscript received 6 November 2000; published 7 March 2001)

Raman scattering under hydrostatic pressure is used to investigate the phonon modes of self-organized Ge quantum dots (QD's) grown by solid source molecular-beam epitaxy. The pressure dependence of Ge-Ge phonon and Si acoustical-overtone (2TA) modes are studied from 0 to 67 kbar at room temperature. Our results show that the overlapping spectra of the Ge-Ge phonon and Si 2TA modes occur around 303 cm^{-1} at ambient pressure which can be resolved at relatively low pressure of about 3 kbar. The linear pressure coefficient of Ge-Ge phonon mode in QD's is found to be $0.29\text{ cm}^{-1}/\text{kbar}$, which is slightly smaller than the corresponding quantity in bulk Ge.

DOI: 10.1103/PhysRevB.63.121306

PACS number(s): 78.66.Db, 78.30.Am

In recent years the spontaneous formation of Ge islands on Si(001) surfaces has attracted considerable attention since the material combination constitutes a model system to study a variety of fundamental nucleation phenomena in the Stranski-Krastanov growth mode.¹⁻⁵ Information on the exact shapes and sizes of nanostructures on a surface is relatively easy to obtain and deep insight has been gained on many aspects of the islands' formation process.¹⁻⁵ For any optoelectronic^{6,7} or electronic^{6,8} applications, though, Ge islands must be overgrown with Si. The shape of the islands can change dramatically during this overgrowth step^{3,9} and only little is known about the resulting islands' strain and composition state. One of the most powerful methods to access information on strain in embedded nanostructures is Raman scattering spectroscopy.

There has been a great deal of effort made, where Raman scattering spectroscopy has been used to study the phonon modes in single-layered Ge dots,^{2,4,10-13} Ge multilayered dots⁵ as well as Ge dot superlattices,¹⁴⁻¹⁶ to predict the phonon confinement and strain effects due to size dependence at ambient pressure. Raman scattering at high pressure offers an attractive means for investigating phonon properties of solids. Besides the reduction of atomic spacing, the effect of pressure will also reduce the strain in Ge layers due to the difference between the bulk moduli of Si and Ge. Although Raman studies on the effect of hydrostatic pressures have been reported on optical phonon of bulk Ge,^{17,18} Si-Ge alloy,¹⁹ $\text{Si}_{1-x}\text{Ge}_x$ superlattices,²⁰ and Ge_nSi_m monolayer superlattices (MLS),²¹ there has been no investigation of Raman studies in Ge QD's under pressure. Hence, in this paper, we report the results of Raman scattering of self-organized Ge QD's under hydrostatic pressure.

The sample for Raman investigations was grown by solid source molecular-beam epitaxy on n^- -Si(001) substrates and undergoes the following growth procedure: Deoxidation at 900°C , growth of a $\sim 400\text{ nm}$ Si buffer layer while ramping the growth temperature down to 500°C , followed by 7 monolayers (ML) Ge and a 160 nm thick Si cap layer. A growth interruption of 5 s is introduced between the Ge and Si layers. Typical growth rates of 1.2 and $0.07\text{ \AA}/\text{s}$ are used for Si and Ge respectively.^{5,13} The sample for atomic-force

microscopy (AFM) follows an almost identical growth procedure except that the Si cap layer is left out and the Ge deposition is 5.8 ML instead of 7 ML.

Figure 1 shows a $0.8 \times 0.8\text{ }\mu\text{m}^2$ AFM scan of nominally 5.8 ML, Ge quantum dots grown at 500°C . The image reveals very small pyramidlike Ge islands (so-called "hut clusters") of diameters $\sim 20\text{ nm}$. This is consistent with the fact that large pyramids and domes usually form at high temperatures, whereas the much smaller hut clusters nucleate at lower temperature.¹³

Pressure-dependent measurements were carried out using a gasketed diamond-anvil cell (DAC). The pressure medium is a 4:1 methanol/ethanol mixture. In order to accommodate the limited dimensions of the space available in the DAC, a small sample with dimensions of $\sim 100 \times 100 \times 30\text{ }\mu\text{m}^3$ was prepared by mechanical polishing and cutting. The applied pressures were determined by the standard method of monitoring the shift of the ruby R1 line.²² Micro-Raman light-scattering experiments were performed in backscattering geometry at room temperature using the 488 nm line from an argon-ion laser. The scattered light was passed through a holographic notch filter, and then analyzed using a 1-m spec-

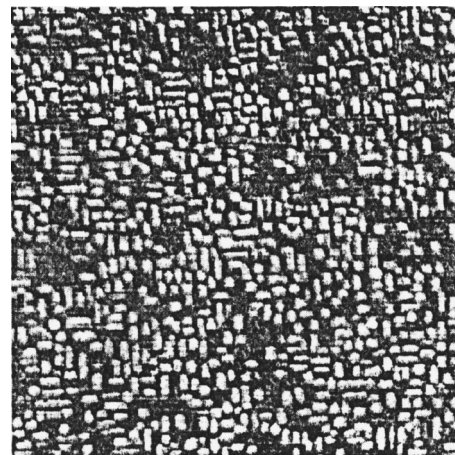


FIG. 1. A $0.8 \times 0.8\text{ }\mu\text{m}^2$ AFM scan of a 6 ML Ge QD's layer grown silicon substrate at 500°C .

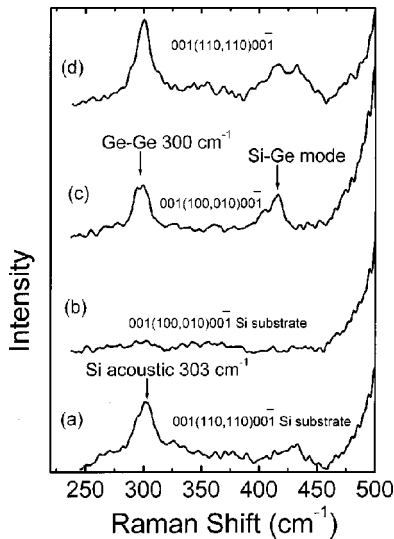


FIG. 2. Raman spectra of the sample and the substrate under different polarization configurations: (a) substrate: $001(110,110)00\bar{1}$, (b) substrate: $001(100,010)00\bar{1}$, (c) sample: $001(100,010)00\bar{1}$, and (d) sample: $001(110,110)00\bar{1}$.

trometer equipped with liquid-nitrogen-cooled multichannel CCD detector. The signal collection time of about 30 min is used for the measurement.

We have used different polarization configurations according to selection rules to distinguish the signals from the dot sample and the Si substrate. A similar approach has been employed in Ref. 23. All the spectra were taken with the same data accumulation time. Figure 2(a) shows the spectrum taken from the Si substrate in the $001(110,110)00\bar{1}$ backscattering geometry as to enhance the Si acoustic phonon peak at $\sim 303\text{ cm}^{-1}$. As expected the Si acoustic phonon peak is suppressed in the $001(100,010)00\bar{1}$ backscattering geometry as illustrated in Fig. 2(b). Figure 2(c) shows the spectrum recorded in the $001(100,010)00\bar{1}$ backscattering geometry from the sample as to minimize the Si acoustic phonon peak. The fact that the line shape and the intensity of the peak at $\sim 300\text{ cm}^{-1}$ from the sample [Fig. 2(c)] are quite similar to the acoustic-phonon peak from the Si substrate [Fig. 2(a)], makes it hard to conclude whether the peak at $\sim 300\text{ cm}^{-1}$ in Fig. 2(c) is due to Ge-Ge mode in the QD's. Figure 2(d) shows the spectrum taken in the $001(110,110)00\bar{1}$ backscattering geometry from the sample in order to enhance the Si acoustic phonon peak. The integrated intensity of the peak at $\sim 301\text{ cm}^{-1}$ is about a factor of 2 stronger than the peak observed at 300 cm^{-1} in Fig. 2(c). We may conclude that the Ge-Ge Raman line from the quantum dot sample contains the contribution from the Si acoustic phonons. In addition, we argue that the Ge-Ge modes are mainly from their Ge dots rather than their Ge wetting layers. This is because in the $001(100,100)00\bar{1}$ configuration, the signals from the Ge wetting layers are forbidden according to the selection rules.²⁴ This point is confirmed by the fact that in this configuration, we found the intensity of Ge-Ge mode in our sample does not change much compared with that in the $001(100,010)00\bar{1}$ configuration.

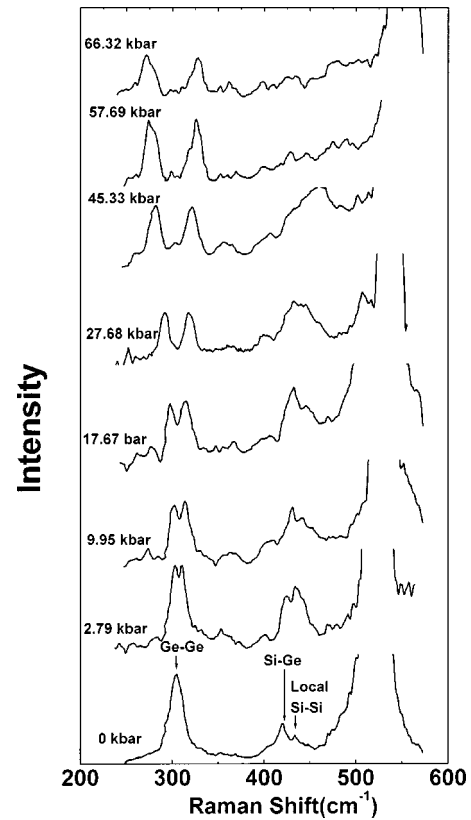


FIG. 3. Room-temperature Raman spectra at various pressures for the Ge QD's taken in the $001(100,-)00\bar{1}$ configuration.

Figure 3 shows the Raman spectra of Ge QD's measured at various pressures up to 67 kbar. At ambient pressure, the sharp peak at 521 cm^{-1} (linewidth limited by the spectrometer resolution) has the same frequency as that of optical phonon peak in bulk Si. The broader peak at 303 cm^{-1} is tentatively assigned to Ge-Ge vibrational mode in QD's and its integrated intensity is over an order of magnitude weaker than the intensity of Si (521 cm^{-1}). The peak at 419 cm^{-1} may be due to Si-Ge interface phonon mode localized at the surfaces of the Ge quantum structures¹⁶ or could possibly be due to Si-Ge intermixing in the islands.^{2,4,10,11} In our case, the islands are grown at relatively low temperatures $\sim 500\text{ }^\circ\text{C}$, and therefore the strain-driven alloying of Ge clusters may not be very pronounced.⁴ The exact value for the degree of intermixing is not available. However, it is likely that there is more than 70% Ge in the dots. In addition, the Si-Si vibrational mode seen at 435 cm^{-1} suggests the existence of strain in Si underneath of the dots induced by the Ge dots.¹⁵ With increasing pressure, the first-order Si Raman peak shifts to higher frequencies with a pressure coefficient of $0.52\text{ cm}^{-1}\text{ kbar}^{-1}$, which (see Fig. 4) can be used as an internal measure of the pressure.²⁵

It has been shown above and also reported by several authors^{20,21,23,26} that the peak at $\sim 303\text{ cm}^{-1}$ could be made up of contributions from the Ge-Ge phonon mode and the Si acoustic-phonon mode. At ambient pressure, these two phonon modes are hardly resolved, as shown in Fig. 3. As pressure increases, the spectrum at $\sim 303\text{ cm}^{-1}$ appears to "split" into two peaks. Pressure causes the lower wave-

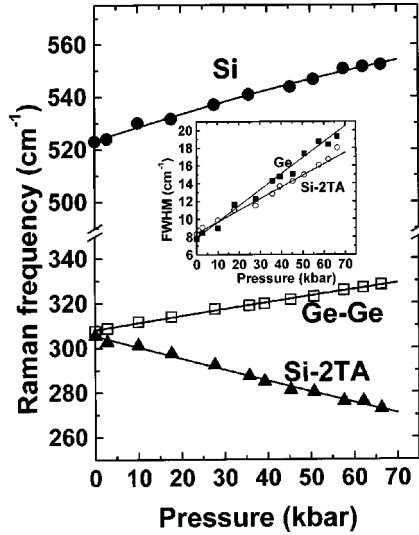


FIG. 4. Raman shifts as function of pressures for Si substrate (solid circles), Ge-Ge mode (open squares) and Si-2TA mode (solid triangles). The solid lines correspond to the quadratic fits to the experimental data. The inset shows the Ge linewidth (solid squares) and Si-2TA mode (open circles) as functions of pressures and the solid lines correspond to the linear fits to the experimental data.

number peak to redshift and the higher wave-number peak to blueshift. At higher pressure, the two peaks are clearly separated. We identify the higher peak to be due to Ge-Ge phonon mode ω_{Ge} from the QD's and attribute the lower peak to acoustical overtone 2TA(X) and possibly, 2TA(Σ) phonons, $\omega_{\text{Si-2TA}}$, (abbreviated as Si-2TA) in Si.²⁵ We have made a deconvolution of these two peaks in order to obtain their peak positions and linewidths as a function of pressure. The results are shown in Fig. 4. Solid lines represent least-squares fit of quadratic functions to the data as given by Eqs. (1) and (2):

$$\omega_{\text{Ge}}(p) = (308.5 \pm 0.4) + (0.29 \pm 0.03)p + (0.2 \pm 0.4) \times 10^{-4} p^2, \quad (1)$$

$$\omega_{\text{Si-2TA}}(p) = (306 \pm 1) - (0.52 \pm 0.05)p + (3.7 \pm 0.7) \times 10^{-4} p^2, \quad (2)$$

where p is in kbars and the frequencies ω are measured in cm^{-1} . The inset in Fig. 4 shows the linewidths Γ of Ge-Ge phonon and Si-2TA phonon modes as a function of pressure. The fitted linear relations for Γ in cm^{-1} are given by

$$\Gamma_{\text{Ge}}(p) = (7.9 \pm 0.4) + (0.177 \pm 0.008)p, \quad (3)$$

$$\Gamma_{\text{Si-2TA}}(p) = (8.4 \pm 0.2) + (0.135 \pm 0.006)p. \quad (4)$$

Our results show that the Ge-Ge phonon frequency in Ge QD's is $\sim 308.5 \text{ cm}^{-1}$ at 0 kbar as compared with that from bulk Ge at 300 cm^{-1} . A blue shift of 8.5 cm^{-1} indicates the presence of compressive strain in the Ge QD's due to the lattice mismatch between Ge and Si. It is known that the Ge-Ge phonon frequency in QD's or nanocrystals can be shifted by phonon confinement in addition to strain effects.

The compressive strain leads to an upward shift of the Ge-Ge mode, while phonon confinement effect leads to a downward shift.²⁷ If we assume the phonon confinement effects are negligible in the Ge QD's, then a biaxial strain²⁸ of about 2.1% is needed for a Raman shift of 8.5 cm^{-1} . For pseudomorphically grown Ge on Si substrate, the compressive strain in the Ge layer is nominally equal to 3.8% which is the lattice mismatch between Si and Ge. In quantum dot structures, this lattice-mismatch-induced strain is partially reduced and non-uniform across the structure as a result of island formation.¹¹

We note that Seon *et al.*²¹ have observed similar effects of hydrostatic pressure in resolving the Ge-Ge mode and Si-2TA mode in the $\text{Ge}_n\text{Si}_m\text{MLS}$, at a pressure > 16 kbar, under off-resonant condition with the E_1 transition in Ge. The intensity of the Si-2TA is weaker than the Ge-Ge mode for all the pressures up to 67 kbar in their case. Our results in Fig. 3 show that the two peaks can be resolved at relatively low pressures (< 3 kbar), and the intensities of the Ge-Ge mode and the Si-2TA are about the same for pressures up to 66 kbar. In the case of MSL, the stress in Ge layers is biaxial in nature with elongation along the growth direction. On the other hand, the quantum dots are compressed along all the three directions similar to that of an applying a hydrostatic pressure. Thus, the presence of a higher degree of compressive strain in QD's as compared to MLS at ambient pressure could facilitate the separation of the two peaks in the Ge QD's when a relatively small pressure is applied.

The pressure coefficient ($\alpha = 0.29 \text{ cm}^{-1} \text{ kbar}^{-1}$) for the Ge-Ge mode frequency in the QD's is found to be slightly smaller than in the bulk Ge ($\alpha = 0.402 \text{ cm}^{-1} \text{ kbar}^{-1}$).¹⁷ This can be explained as follows. The in-plane lattice constant of Ge layers is compressed to match with that of the surrounding Si. Since Ge has a smaller bulk modulus than Si, the Ge layers will show a smaller change in the in-plane lattice constant than the Si for a given applied pressure. This is expected to happen in $\text{Ge}_n\text{Si}_m\text{MLS}$.²¹ Additionally, we expect a further reduction of strain in the Ge QD's since the lattice dilation for the Ge layers along the growth direction will also be constrained by the surrounding Si. Therefore, the Ge QD's will exhibit a much smaller deformation than the bulk Ge as well as the $\text{Ge}_n\text{Si}_m\text{MLS}$, when subjected to the same pressure. The appearance of Si-2TA mode is possibly due to strain in the Si layer around the Ge dots.²³

It is noteworthy that the linewidth of the Si-Ge mode, observed at 419 cm^{-1} in Fig. 3 at ambient pressure, broadens and the peak blueshifts with pressure. Unfortunately, we are unable to give a quantitative analysis on this peak as the signal becomes smeared out and buried under noise at high pressure. This could be due to inhomogeneous strain at the Ge/Si interface of the QD's.

In summary, effects of pressure on the Raman spectrum of Ge QD's are examined. Pressure-induced phonon shifts clearly resolved the Ge-Ge mode in QD's and Si acoustic mode at relatively low pressure. Our results show that strain is the dominant effect in the Ge QD's. The pressure coefficient for the Ge-Ge mode frequency in QD's is smaller than the corresponding quantity in bulk Ge.

- *Corresponding author. Email address: eleteokl@nus.edu.sg
- ¹J. A. Floro, M. B. Sinclair, E. Chason, L. B. Freund, R. D. Twes-ten, R. Q. Hwang, and G. A. Lucadamo, *Phys. Rev. Lett.* **84**, 701 (2000); D. E. Jesson, M. Kastner, B. Voigtlander, *ibid.* **84**, 330 (2000); M. Kastner, and B. Voigtlander, *ibid.* **82**, 2745 (1999); G. Wedler, J. Walz, T. Hesjedal, E. Chilla, and R. Koch, *ibid.* **80**, 2382 (1998); F. M. Ross, J. Tersoff, and R. M. Tromp, *ibid.* **80**, 984 (1998); I. Goldfarb, P. T. Hayden, J. H. G. Owen, G. A. D. Briggs, *ibid.* **78**, 3959 (1997); A. J. Steinfert, P. M. L. O. Scholte, A. Ettema, F. Tuinstra, M. Nielsen, E. Landemark, D. M. Smilgies, R. Feidenhansl, G. Falkenberg, L. Seehofer, and R. L. Johnson, *ibid.* **77**, 2009 (1996).
 - ²Chuan-Pu Liu, J. Murray Gibson, David G. Cahill, Theodore I. Kamins, David P. Basile, and R. Stanley Williams, *Phys. Rev. Lett.* **84**, 1958 (2000).
 - ³O. G. Schmidt and K. Eberl, *Phys. Rev. B* **61**, 13 721 (2000).
 - ⁴S. A. Chaparro, J. Drucker, Y. Zhang, D. Chandrasekhar, M. R. McCartney, and D. J. Smith, *Phys. Rev. Lett.* **83**, 1199 (1999).
 - ⁵O. G. Schmidt, O. Kienzle, Y. Hao, K. Eberl, and F. Ernst, *Appl. Phys. Lett.* **74**, 1272 (1999); O. Kienzle, F. Ernst, M. Rühle, O. G. Schmidt, and K. Eberl, *ibid.* **74**, 269 (1999).
 - ⁶K. Eberl, O. G. Schmidt, R. Duschl, O. Kienzle, F. Ernst, and Y. Rau, *Thin Solid Films* **369**, 33 (1999).
 - ⁷L. Vescan, T. Stoica, *J. Lumin.* **80**, 485 (1998).
 - ⁸K. Eberl, O. G. Schmidt, O. Kienzle, and F. Ernst, *Solid State Phenom.* **69-70**, 13 (2000); O. G. Schmidt and K. Eberl, German Patent No. 100 25 264.8 (22 May 2000).
 - ⁹O. G. Schmidt, U. Denker, K. Eberl, O. Kienzle, and F. Ernst, *Appl. Phys. Lett.* **77**, 2509 (2000); M. Kummer, B. Vögli, and H. v. Känel, *Mater. Sci. Eng., B* **69-70**, 247 (2000); P. Sutter and M. G. Lagally, *Phys. Rev. Lett.* **81**, 3471 (1998).
 - ¹⁰F. Boscherini, G. Capellini, L. Di Gaspare, F. Rosei, N. Motta, and S. Mobilio, *Appl. Phys. Lett.* **76**, 682 (2000).
 - ¹¹V. Magidson, D. V. Regelman, R. Beserman, and K. Dettmer, *Appl. Phys. Lett.* **73**, 1044 (1998).
 - ¹²J. Groenen, R. Carles, S. Christiansen, M. Albrecht, W. Dorsch, H. P. Strunk, H. Wawra, and G. Wagner, *Appl. Phys. Lett.* **71**, 3856 (1997); P. D. Persans, P. W. Deelman, K. L. Stokes, L. J. Schowalter, A. Byrne, and T. Thundat, *ibid.* **70**, 472 (1997); C. E. Bottani, C. Mantini, P. Milani, M. Manfredini, A. Stella, P. Tognini, P. Cheyssac, and R. Kofman, *ibid.* **69**, 2409 (1996).
 - ¹³O. G. Schmidt, C. Lange, and K. Eberl, *Appl. Phys. Lett.* **75**, 1905 (1999).
 - ¹⁴J. L. Liu, G. Jin, Y. S. Tang, Y. H. Luo, K. L. Wang, and D. P. Yu, *Appl. Phys. Lett.* **76**, 586 (2000).
 - ¹⁵J. L. Liu, Y. S. Tang, K. L. Wang, T. Radetic, and R. Gronsky, *Appl. Phys. Lett.* **74**, 1863 (1999).
 - ¹⁶S. H. Kwok, P. Y. Yu, C. H. Tung, Y. H. Zhang, M. F. Li, C. S. Peng, and J. M. Zhou, *Phys. Rev. B* **59**, 4980 (1999).
 - ¹⁷C. Ulrich, A. Debernardi, E. Anastassakis, K. Syassen, and M. Cardona, *Phys. Status Solidi B* **211**, 293 (1999); C. Ulrich, E. Anastassakis, K. Syassen, A. Debernardi, and M. Cardona, *Phys. Rev. Lett.* **78**, 1283 (1997).
 - ¹⁸D. Olego and M. Cardona, *Phys. Rev. B* **25**, 1151 (1982).
 - ¹⁹Zhifeng Sui, Hubert H. Burke, and Irving P. Herman, *Phys. Rev. B* **48**, 2162 (1993).
 - ²⁰S. Hitomi, K. Takarabe, S. Minomura, J. Sakai, and T. Tatsumi, *J. Phys. Chem. Solids* **56**, 292 (1995).
 - ²¹M. Seon, M. Holtz, Ta-Ryeong Park, O. Brafman, and J. C. Bean, *Phys. Rev. B* **58**, 4779 (1998).
 - ²²G. J. Piermarini, S. Block, J. D. Barnett, and R. A. Forman, *J. Appl. Phys.* **46**, 2774 (1975).
 - ²³J. L. Liu, G. Jin, Y. S. Tang, and K. L. Wang, *Appl. Phys. Lett.* **75**, 3574 (1999).
 - ²⁴R. Schorer, G. Abstreiter, S. de Gironcoli, E. Molinari, H. Kibbel, and H. Presting, *Phys. Rev. B* **49**, 5406 (1994).
 - ²⁵Bernard A. Weinstein, and G. J. Piermarini, *Phys. Rev. B* **12**, 1172 (1975).
 - ²⁶A. V. Kolobov and K. Tanaka, *Appl. Phys. Lett.* **75**, 3572 (1999); A. V. Kolobov, *J. Appl. Phys.* **87**, 2926 (2000).
 - ²⁷P. M. Fauchet and I. H. Campbell, *CRC Crit. Rev. Solid State Mater. Sci.* **14**, S79 (1988).
 - ²⁸F. Cerdeira, A. Pinczuk, J. C. Bean, B. Batlogg, and B. A. Wilson, *Appl. Phys. Lett.* **45**, 1138 (1984).